Microstructure and conductivity of hierarchical laminate composites

J. Quintanilla* and S. Torquato†
Princeton Materials Institute and Department of Civil Engineering and Operations Research, Princeton, New Jersey 08544
(Received 30 October 1995)

Certain hierarchical laminates with a wide separation of length scales are known theoretically to have optimal transport and mechanical properties. We derive analytical expressions for the n-point probability functions that statistically characterize the microstructure for more general hierarchical laminates with an arbitrary number of stages and a finite separation of length scales. Using two-point probability information, we rigorously bound the effective conductivity (or dielectric constant) tensor for macroscopically anisotropic laminates and study how the separation of length scales affects the effective properties.

PACS number(s): 05.20.−y, 03.20.+i

I. INTRODUCTION

Since the details of the microstructure of random materials are usually not completely known, researchers have, in lieu of an exact determination, either estimated or bounded the effective properties of random materials given limited microstructural information [1,2]. One interesting problem in the case of bounding approaches is finding the microstructures that saturate the bounds, i.e., determining the optimal microstructures. Certain laminate composites with structural hierarchy (structure at different length scales) are known to optimize the effective conductivity [3–6] as well as the effective elastic moduli [5–11]. Hierarchical composites are also of practical interest since they are abundant in nature [12]: tendon [13], bone [14], and mollusk shells [15] are excellent examples of hierarchical biological composites.

To our knowledge, the quantitative characterization of the microstructure (via statistical correlation functions) of hierarchical laminates has been lacking. Moreover, there are presently no rigorous estimates of the effective properties of hierarchical laminates when the separation between the length scales is finite. In this paper, we will address these issues in the context of finding the effective conductivity tensor of such materials.

In Fig. 1 we show a portion of a random laminate of *second rank*, i.e., one that possesses two levels of hierarchy. It is constructed in two stages. The first stage is simply a series of parallel strips of width d_1 in the x direction generated by some one-dimensional random process. For this process we define $\phi_1^{(1)}$ and $\phi_2^{(1)}$ to be the volume fractions of the disconnected phase (phase 1) and the ''slab'' phase (phase 2), respectively. We also respectively define σ_1 and σ_2 to be the conductivities of phases 1 and 2. The second stage of lamination adds perpendicular strips of width d_2 in the gaps of the first stage. We define $\phi_1^{(2)}$ and $\phi_2^{(2)}$ to be the volume fractions of phases 1 and 2 for the second-stage processes, respectively. Clearly from this construction

$$\phi_1^{(1)}+\phi_2^{(1)}=\phi_1^{(2)}+\phi_2^{(2)}=1. \tag{1}$$

Also, a point lies in phase 1 of the entire laminate exactly when its x coordinate lies in phase 1 of the first stage and its y coordinate lies in phase 1 of the second stage of lamination. Since these events are independent, we see that the volume fraction of phase 1 of the entire laminate is given by

$$\phi_1=1-\phi_2=\phi_1^{(1)}\phi_1^{(2)}. \tag{2}$$

By repeating this procedure one can create higher-rank laminates in the plane. We also can generalize this procedure to higher dimensions, although we restrict our attention to two dimensions in this paper. Finally, laminates in general do not necessarily need to have orthogonal stages; we only consider such laminates in this paper to facilitate our characterization of the microstructure. We will discuss how to apply our microstructural characterization to laminates without orthogonal stages.

Typical one-dimensional systems from which laminates are constructed are fully penetrable rods, totally impenetrable rods in thermal equilibrium, and one-dimensional ''random checkerboards.'' Realizations of these three systems are shown in Fig. 2; the systems depicted have equal rod lengths and volume fractions of the phases. Notice that the clusters could have width larger than d in the systems which permit the individual rods to overlap. By extending these one-dimensional systems into two dimensions, hierarchical laminates are constructed.

Much research has been conducted on hierarchical laminates with a wide separation of length scales [3–6] (for laminates of second rank, this condition means that d_1/d_2 tends

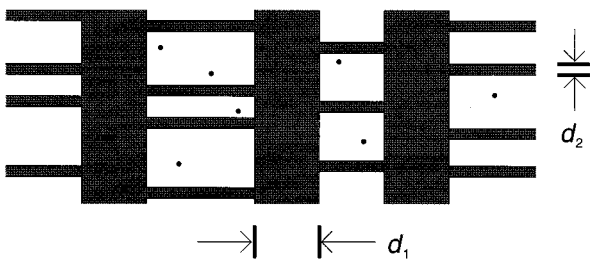

FIG. 1. A portion of a typical second-rank laminate, and one way that seven points could fall within the gaps of the first stage of lamination.

*Electronic address: johnq@matter.princeton.edu
†Electronic address: torquato@matter.princeton.edu

 © 1996 The American Physical Society

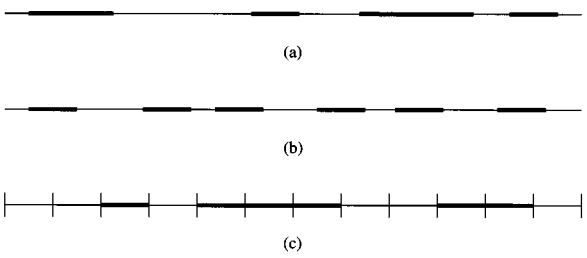

FIG. 2. The three one-dimensional random systems considered in this paper: (a) fully penetrable rods, (b) totally impenetrable rods, and (c) a one-dimensional random checkerboard process. The rods of the three systems have a common width d; however, the clusters in systems (a) and (c) can be longer than d due to overlap. Laminates are generated by extending such systems into two-dimensional systems of gaps and slabs.

to infinity). For such laminates, the fields are piecewise uniform within the two phases of the composite, and so exact expressions for the effective properties can be obtained by using macroscopic methods. However, laminates with only a finite separation of length scales do not have piecewise uniform fields, and for this reason the macroscopic properties of such laminates cannot be calculated analytically. Some other technique must be employed to estimate or bound the effective properties.

To study laminates with a finite separation of length scales, we will use contrast expansion theory, which was formulated by Sen and Torquato [16,17]. They derived the following series expansion for the effective conductivity tensor $\boldsymbol{\sigma}_e$ for any d-dimensional two-phase random composite (in particular, random laminates):

$$(\phi_i\beta_{ij})^2(\boldsymbol{\sigma}_e-\sigma_j\mathbf{I})^{-1}[(\boldsymbol{\sigma}_e+(d-1)\sigma_j\mathbf{I}] = \phi_i\beta_{ij}\mathbf{I}-\sum_{n=2}^{\infty}\mathbf{A}_n^{(i)}\beta_{ij}^n, \tag{3}$$

where $\mathbf{I}$ is the identity tensor, $i,j=1,2,\ i\neq j$,

$$\beta_{ij}=\frac{\sigma_i-\sigma_j}{\sigma_i+(d-1)\sigma_j}, \tag{4}$$

and the tensor coefficients $\mathbf{A}_n^{(i)}$ are functionals of $S_1,\ldots,S_n$, where $S_p(\mathbf{r}^p)$ is the probability that p given points $\mathbf{r}^p\equiv\mathbf{r}_1,\ldots,\mathbf{r}_p$ all lie within phase i. (Bounds of arbitrary order can be obtained from (3); this will be discussed later.) Unlike the other tensor coefficients, $\mathbf{A}_2^{(1)}=\mathbf{A}_2^{(2)}$, and henceforth their common value will be denoted by $\mathbf{A}_2$. In two dimensions $\mathbf{A}_2$ is traceless and is explicitly given by

$$\mathbf{A}_2=\frac{1}{\pi}\lim_{\delta\to 0}\int_{\delta}^{\infty}\frac{dr}{r}\int_0^{2\pi}d\theta\begin{bmatrix}\cos 2\theta & \sin 2\theta\\ \sin 2\theta & -\cos 2\theta\end{bmatrix} \times[S_2(r,\theta)-\phi_1^2] \tag{5}$$

for statistically homogeneous media; see Ref. [16] for the integral expressions for the higher $\mathbf{A}_n^{(i)}$. The quantity (r,θ) in the integrand represents the separation between the two points that lie in phase 1 in polar coordinates.

If we omit the series in (3), we obtain the well-known Hashin-Shtrikman bounds on the effective conductivity of isotropic two-phase composites in two and three dimensions [18]. These bounds are the best possible given only volume-fraction information, and hence *optimal*, since they can be realized for several classes of composites [3,4,18,19]. One such class of optimal structures (i.e., structures that achieve these bounds) are macroscopically isotropic laminates, which have a wide separation of length scales and satisfy the volume fraction requirement [3,4]

$$\phi_2^{(1)}=\phi_2^{(2)}/\phi_1^{(2)}. \tag{6}$$

For macroscopically isotropic laminates, the tensor coefficients $\mathbf{A}_n^{(i)}$ must vanish [6].

If S_2 is independent of the direction θ (statistical isotropy), or is symmetric about the line $\theta=\pi/4$, then $\mathbf{A}_2$ is trivially zero in view of (5). However, from geometrical considerations (elaborated in Sec. II), S_2 is inherently statistically anisotropic for the hierarchical laminate of Fig. 1 and thus obeys neither of these symmetries, yet $\mathbf{A}_2$, as shall be shown, vanishes anyway when the laminate is macroscopically isotropic. To demonstrate this, we will first calculate the microstructure function S_2 for laminates and then use (5) to explicitly show, from the microstructure, that $\mathbf{A}_2=\mathbf{0}$ for macroscopically isotropic laminates.

By taking certain Padé approximants of (3), Sen and Torquato obtained bounds of arbitrary order on the effective conductivity tensor in terms of the $\mathbf{A}_n^{(i)}$, which in turn depend on the S_n [16]. In this paper we will study the second-order bounds obtained from a [1,1] Padé approximant of (3). The bounds on the effective conductivity in the two principal directions are identical and equal to the Hashin-Shtrikman bounds whenever $\mathbf{A}_2=\mathbf{0}$. However, when $\mathbf{A}_2$ is not equal to the zero tensor, the two sets of bounds are not identical but instead are directionally dependent. Therefore, when we take laminates which satisfy (6) and have an increasing separation of length scales, the bounds in the two principal directions both converge to the Hashin-Shtrikman bounds. Approaching laminates from the perspective of their microstructure therefore allows us to study how the separation of length scales (i.e., the nonuniformity of the fields within the phases) affects the effective conductivity tensor.

Summarizing, in this paper we study the following questions: What are the S_n for laminates with any separation of length scales? Does the functional behavior of S_n reflect the construction of the laminate? Can we bound the effective conductivity of laminates with a finite separation of length scales? How does the separation of length scales affect these bounds? How close are they to the bounds for laminates with an infinite separation of length scales? Are these results in agreement with known results as the separation of length scales tends to infinity? Finally, one outstanding unsolved problem: what are all classes of optimal composites; i.e., what form must the S_n have so that the $\mathbf{A}_n^{(i)}$ vanish? A study of the microstructure of laminates may provide a first step toward answering this difficult last question.

In Sec. II we obtain analytical representations of the S_n for fully penetrable laminates of arbitrary rank and S_2 for laminates of arbitrary rank and construction in terms of the microstructure of the one-dimensional generating processes.

We explicitly calculate S_2 for second-rank fully penetrable laminates, totally impenetrable laminates, and laminates generated by random checkerboards. Our expressions are valid for laminates with a finite separation of length scales. In Sec. III we use our expression for S_2 to calculate the two-point tensor coefficient $\mathbf{A}_2$ and therefore bounds on $\boldsymbol{\sigma}_e$ for laminates with a finite separation of length scales. We then let the separation of length scales tend to infinity and verify that the bounds in the two principal directions indeed both converge to the Hashin-Shtrikman bounds for macroscopically isotropic hierarchical laminates.

II. MICROSTRUCTURE OF LAMINATES

To begin, we study the microstructure of laminates in the plane. We first define the n-point phase 1 probability functions S_n and the lineal path function L. These functions are inherently anisotropic for laminates since the laminates themselves are statistically anisotropic. We develop a recursive equation valid for any S_n for random laminates of arbitrary rank generated by systems of fully penetrable rods. Generalizations are then discussed, including an expression for S_2 for laminates of arbitrary rank and construction; this expression will be used in our numerical calculations of $\mathbf{A}_2$ in Sec. III. We then use this expression to calculate S_2 for three types of second-rank laminates: fully penetrable laminates, totally impenetrable laminates, and laminates generated by random checkerboards. Finally, we study how S_2 reflects the structure of laminates on their multiple length scales. (In Appendix A we will consider the lineal path function for second-rank laminates.)

A. Definitions of microstructure functions

The probability that n points with positions $\mathbf{r}^n$ all lie in phase 1 is denoted by $S_n(\mathbf{r}^n)=\mathbf{r}_1, \ldots, \mathbf{r}_n$ and can be explicitly written as [20]

$$S_n(\mathbf{r}^n)=\left\langle \prod_{j=1}^{n} I(\mathbf{r}_j) \right\rangle, \tag{7}$$

where I is the indicator function of phase 1; i.e.,

$$I(\mathbf{r})=\begin{cases} 1, & \mathbf{r} \text{ in phase 1,} \\ 0, & \text{otherwise.} \end{cases} \tag{8}$$

The angular brackets denote an ensemble average over the possible realizations. For statistically homogeneous media, the S_n are dependent only on the relative displacements so that, for example, $S_1 = \phi_1$, the volume fraction of phase 1.

When we refer to the microstructure of laminates in this paper, S_n will denote the microstructure function for the full laminate. We also define $S_n^{(i)}$ to be the n-point probability function for phase 1 for the one-dimensional process which determines the ith stage of lamination.

The probability that a vector $\mathbf{x}$ is wholly contained in phase 1 is called the lineal path function [21] and is denoted by $L(\mathbf{x})$. This probability is different than S_2, which requires that only the endpoints of the line lie in the same phase. We also define $L^{(i)}$ to be the one-dimensional lineal path function for the process which determines the ith stage of lamination.

We now characterize the microstructure of laminates by calculating S_n in terms of the functions $S_n^{(i)}$ and $L^{(i)}$.

B. S_n for fully penetrable laminates of arbitrary rank

By a *fully penetrable laminate*, we mean a laminate generated by fully penetrable (i.e., spatially uncorrelated) rods at each stage of lamination, so that the ith stage of lamination is probabilistically determined by the width of the laminates d_i and the number density of lamination ρ_i. We allow the possibility that the strips overlap in general, so that the ''slabs'' generated by the strips of the ith stage may have width greater than d_i. We also assume the processes of the ith stage of lamination are identically distributed and independent both of each other and the processes of every other stage of lamination. This assumption also holds for the more general laminates considered later in this paper.

To calculate the probability that n points $\mathbf{r}_1, \mathbf{r}_2, \ldots, \mathbf{r}_n$ all fall in the disconnected phase of a kth-rank fully penetrable laminate, we first order the n points by their x-coordinates so that $x_1 \leqslant x_2 \leqslant \cdots \leqslant x_n$. We then use a key property of random laminates: the laminates of order $k-1$ embedded in the gaps of the first stage of lamination are generated *independently* of each other.

To utilize this feature, we introduce some notation to enumerate the 2^{n-1} different ways that the ordered n points could fall into the gaps of the first stage of lamination. Consider the set A of n-tuples of the letters 0 and 1 whose nth element is 1. Then there is a one-to-one correspondence between the elements of this set and the permutations of the n points in different gaps: if $p_0=0$ and $p_1, \ldots, p_m$ are the positions of the 1s in an element a of A, we associate with this element a the event that the sets of points $\{x_{p_j+1}, \ldots, x_{p_{j+1}}\}$ fall in the same gap and in a different gap than the set corresponding to any other j. (For brevity we suppress the dependence of the p_j and m on the n-tuple a.) We conclude from this bijection that there are indeed 2^{n-1} ways the ordered points could lie in the gaps.

To illustrate this notation, consider the event of seven points falling in the disconnected phase depicted in Fig. 1. From left to right, the first four points lie in one gap of the first stage of lamination, the next two points lie in another gap, while the last point lies a third gap. The sequence corresponding to this event is $a=\{0,0,0,1,0,1,1\}$, so that $m=3$, $p_0=0$ (as always), $p_1=4$, $p_2=6$, and $p_3=7$ ($p_m=n$ always). Under this construction, $a_l=1$ exactly when point l is the rightmost point in a gap.

Since a Poisson distributed system has independent and stationary increments, the probability that the n points will fall in the gaps of the first stage of lamination according to the arrangement associated with $a \in A$ is

$$P(a)=S_n^{(1)}(x_1, \ldots, x_n) \prod_{l=1}^{n-1} M(x_{l+1}-x_l; a_l), \tag{9}$$

where a_l is the lth element of a,

$$M(r,0)=\frac{L^{(1)}(r)}{S_2^{(1)}(r)}=\begin{cases}1, & r\leqslant d_1,\\ e^{-\rho_1(r-d_1)}, & r>d_1,\end{cases} \tag{10}$$

and

$$M(r,1)=1-M(r,0). \tag{11}$$

The functions S_2 and L for fully penetrable rods are given explicitly in (17) and (18). The calculation of this probability is not so trivial for more general one-dimensional processes, as discussed in the next subsection.

Once we have isolated the x coordinates in the gaps of the first stage of lamination, we must now calculate the probability that the set $\{\mathbf{r}_{p_j+1},\ldots,\mathbf{r}_{p_{j+1}}\}$ (i.e., all the points that lie in an arbitrary gap) also lies in the disconnected phase. Since the processes within the gaps of the first stage are embedded laminates of rank $k-1$ rotated 90° from the usual orientation, this conditional probability is just $S'_{p_j-p_{j-1}}(\mathbf{r}^t_{p_{j-1}+1},\ldots,\mathbf{r}^t_{p_j})$, where $\mathbf{r}^t$ is the transpose of $\mathbf{r}$ and S'_p is the p-point disconnected-phase probability function of the embedded laminates of rank $k-1$.

Since the processes in the embedded laminates are assumed to be independent of each other and the first stage of lamination, we finally conclude using the law of total probability that

$$S_n(\mathbf{r}_1,\ldots,\mathbf{r}_n)=S_n^{(1)}(x_1,\ldots,x_n)\sum_{a\in A}\prod_{l=1}^{n-1}M(x_{l+1}-x_l;a_l)\prod_{j=1}^{m}S'_{p_j-p_{j-1}}(\mathbf{r}^t_{p_{j-1}+1},\ldots,\mathbf{r}^t_{p_j}). \tag{12}$$

Through repeated use of (12) we can reduce S_n for a kth-rank laminate to the one-dimensional functions $S_p^{(i)}$ for $1\leqslant p\leqslant n$ and $1\leqslant i\leqslant k$.

C. S_n for general random laminates

In principle, the above approach could be applied to laminates of arbitrary rank generated by random processes other than fully penetrable rods. However, such a recursive relationship would require knowledge of microstructure functions never before considered in the literature. For example, determining S_3 requires knowing the probability that, given three points, the first two lie in one gap and the third lies in another gap. While such probabilities can be computed explicitly for fully penetrable rods, and is done in (9), they have not been considered for more general one-dimensional systems.

However, the probability that only two points do or do not lie in the same gap is determined by the defined one-dimensional two-point phase 1 probability functions $S_2^{(i)}$ and the lineal path functions $L^{(i)}$, and so S_2 can be calculated for general random laminates of arbitary rank. Our analysis of conditioning of the positions of the two points relative to the first stage of lamination is particularly self-evident in determining S_2 for second-rank laminates of arbitrary construction. If the two x coordinates lie in the same gap, then the y coordinates both must lie in phase 1 of the second-stage one-dimensional process in that gap. On the other hand, if they lie in different gaps, then the two y coordinates need to lie in phase 1 of two independent processes. Using the law of total probability and this analysis, we conclude that

$$S_2(x,y)=L^{(1)}(x)S_2^{(2)}(y)+[S_2^{(1)}(x)-L^{(1)}(x)](\phi_1^{(2)})^2, \tag{13}$$

where (x,y) is the displacement between the two points. The complexity of the general expression (12) is thus greatly simplified when $n=k=2$. Similar expressions for S_2 can be developed for laminates of higher rank. As expected, $S_2(x,y)$ tends to its long-range value of ϕ_1^2 as $x,y\to\infty$. This will be used in the integrations of the next section.

Finally, we can use our analysis to calculate S_n for laminates that do not have orthogonal stages. For example, a second-rank laminate whose second stage is at angle θ from horizontal can be transformed to a topologically equivalent orthogonal laminate via the linear transformation

$$(x,y)\to(x,y-x\,\tan\theta). \tag{14}$$

To calculate S_n for this slanted laminate, we would first project the points to their images under the above transformation and then calculate S_n for this orthogonal laminate.

D. Calculation of S_2 for second-rank laminates

In this section we will use (13) to calculate $S_2(x,y)$ for second-rank fully penetrable laminates, totally impenetrable laminates, and laminates generated by random checkerboards. We will also show that S_2 reflects the behavior of laminates on their multiple length scales.

1. Fully penetrable laminates

We now explicitly state S_2 for fully penetrable second-rank laminates in terms of the generating one-dimensional processes. The microstructure of fully penetrable rods (an example of which is shown in Fig. 2) on a line is very well understood. If the rods have diameter d and number density ρ, and we define the reduced density η by

$$\eta=\rho d, \tag{15}$$

then we have [22]

$$S_1\equiv\phi_1=e^{-\eta}. \tag{16}$$

For two points separated by a distance x, the two-point phase 1 probability function is given by

$$S_2(u)=\begin{cases} e^{-\eta(1+u)}, & u\leq 1, \\ e^{-2\eta}, & u>1, \end{cases} \tag{17}$$

where $u=|x|/d$ is dimensionless distance.

The lineal path function for fully penetrable rods is given by [21]

$$L(u)=e^{-\eta(1+u)}, \tag{18}$$

so that, not surprisingly, $L(u)=S_2(u)$ for $u\leq 1$.

Substitution of these results into (13) and use of dimensionless units $u=|x|/d_1$ and $v=|y|/d_2$ yields

$$S_2(u,v)=\begin{cases} \phi_1 e^{-\eta_1 u-\eta_2 v}, & u\leq 1, v\leq 1, \\ \phi_1 e^{-\eta_1 u-\eta_2}, & u\leq 1, v>1, \\ \phi_1[e^{-\eta_1 u}(e^{-\eta_2 v}-e^{-\eta_2})+\phi_1], & u>1, v\leq 1, \\ \phi_1^2, & u>1, v>1, \end{cases} \tag{19}$$

where η_1 and η_2 are the reduced densities for the first and second stages of lamination, respectively. Notice that S_2 is identically equal to ϕ_1^2 for sufficiently large u and v, just as in the one-dimensional case of fully penetrable rods.

This expression for S_2 matches simulation data as well. In Fig. 3 we plot S_2 for second-rank fully penetrable laminates, where in the x-direction we take $\eta_1=1/4$, while in the y-direction we take $d_2=d_1/2$ and $\eta_2=1/3$. We plot $S_2(w,\theta)$ for $w=0.75$ and $w=2.5$ over $0\leq\theta\leq\pi/2$, where

$$x=r\cos\theta \tag{20}$$

and

$$y=r\sin\theta \tag{21}$$

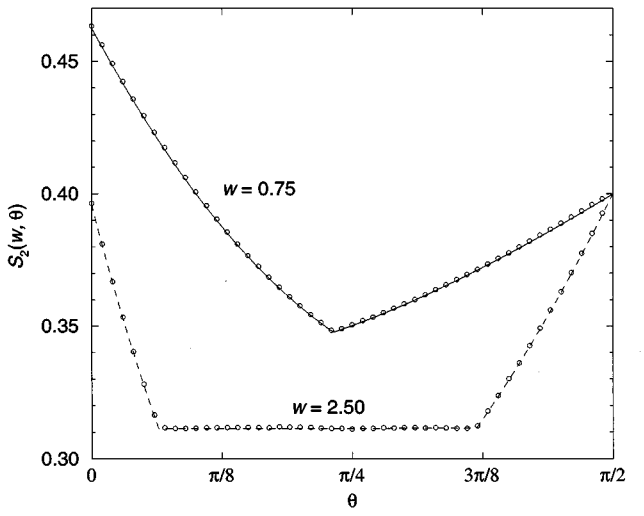

FIG. 3. The two-point probability function $S_2(w,\theta)$ for a second-rank fully penetrable laminate with $d_2=d_1/2$, $\eta_1=1/4$, and $\eta_2=1/3$. Here d_i and η_i are the rod lengths and reduced densities of stage i, respectively. S_2 is shown at dimensionless radial distances $w=r/d_1=0.75$ and $w=2.5$. Computer simulation data are represented by circles. We see that the theoretical expression (19) for S_2 is in excellent agreement with simulation results.

as usual, and $w=r/d_1$. [From geometric considerations, $S_2(w,\theta)$ is symmetric about $\theta=\pi/2$ and is periodic with period π.] As we see, our simulation data is in excellent agreement with (19). We also note that, as expected, S_2 is not symmetric about $\theta=\pi/4$.

2. Totally impenetrable laminates

We now consider second-rank laminates which are constructed by systems of hard rods of equal diameter d in thermal equilibrium. A possible realization of such a system was given in Fig. 2. As before, we need the quantities $S_2^{(i)}(x)$ and $L^{(i)}(x)$ for the one-dimensional processes that generate the laminate to determine S_2 for the full laminate. Torquato and Lado [23] calculated S_2 explicitly for a system of hard rods in equilibrium. After some simplification their expression can be written in terms of the dimensionless distance $u=|x|/d$ as

$$S_2(u)=(1-\eta)\sum_{k=0}^{j}\frac{\exp(-[u-k]/a)}{k!}\left(\frac{u-k}{a}\right)^k, \tag{22}$$

where $j\leq u\leq j+1$ and

$$a=\frac{1-\eta}{\eta}. \tag{23}$$

As before, η is the reduced density. Since the rods do not overlap,

$$\phi_1=1-\eta. \tag{24}$$

For sufficiently large u, $S_2(u)$ can be accurately approximated using the method of subtracted singularities, as explained in Appendix B. This asymptotic approximation will turn out to be useful in numerically computing the tensor coefficient $\mathbf{A}_2$, as described in Sec. III.

Also, Lu and Torquato [21] calculated the lineal path function L exactly for a system of hard rods in equilibrium and found that

$$L(u)=(1-\eta)\exp(-u/a). \tag{25}$$

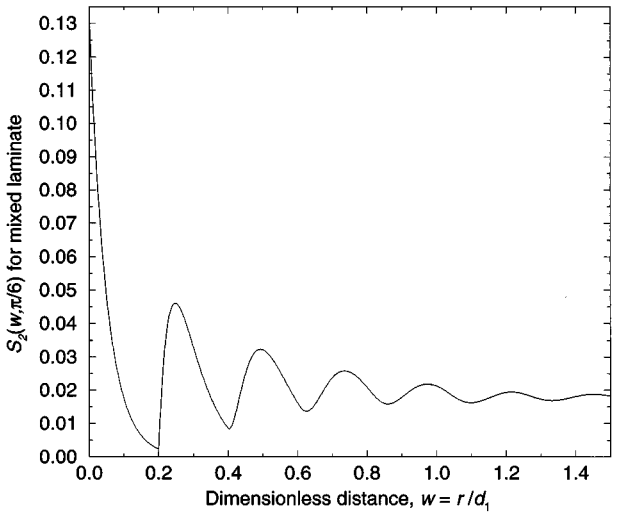

FIG. 4. $S_2(w,\pi/6)$ in a mixed second-rank laminate where again $w=r/d_1$. The first stage is generated by fully penetrable rods with $\eta_1=0.4$. The second stage is generated by totally impenetrable rods in thermal equilibrium with $\eta_2=0.8$ and $d_2=0.1d_1$. As we see, S_2 for this mixed system has characteristics of both systems on the two different length scales.

As before, $L(u)=S_2(u)$ for $u\leqslant 1$.

Therefore, to calculate S_2 for totally impenetrable laminates, we substitute (22) and (25) with appropriate η_1 and η_2 into (13). As with fully penetrable laminates, this expression is also in agreement with computer simulations.

3. Random checkerboard laminates

A third type of laminate is constructed by one-dimensional checkerboard processes, also depicted in Fig. 2, in which the line is divided into equisized sections of width d. Each section, independent of the other sections, belongs to phase 1 with probability ϕ_1 and phase 2 with probability ϕ_2. The required microstructure functions for phase 1 are then given by

$$S_2(u)=\begin{cases}(1-u)\phi_1+u\phi_1^2, & u\leqslant 1,\\ \phi_1^2, & u>1,\end{cases} \tag{26}$$

and

$$L(u)=(1-z)\phi_1^n+z\phi_1^{n+1}, \tag{27}$$

where the dimensionless distance is decomposed as $u=(n-1)+z$ with $0\leqslant z<1$. Substitution of these into (13) gives S_2 for the full laminate. We note that for sufficiently large x and y, $S_2(x,y)$ is identically equal to ϕ_1^2, just as in the case of the one-dimensional checkerboard model.

4. Behavior of S_2 on different length scales

To conclude this section we discuss how the graph of S_2 can reflect the processes which construct the laminate. In particular, we show that S_2 reflects microstructural information about a composite on its different length scales.

In Fig. 4 we plot $S_2(w,\pi/6)$, where again we use polar coordinates with $w=r/d_1$, for a laminate constructed by two different one-dimensional processes. The first stage is generated by a system of fully penetrable rods with $\eta_1=0.4$. The second stage is generated by systems of totally impenetrable rods in thermal equilibrium with $\eta_2=0.8$ and $d_2=0.1d_1$.

As we see, S_2 for this laminate reflects properties of the functional behavior of S_2 for the one-dimensional processes. On the length scale $w=O(1)$, S_2 decays exponentially and then more or less flattens, just like it does for ''pure'' fully penetrable rods [see (17)]. However, on the length scale $w=O(0.1)$, we see a sharp cusp and dampened oscillations, just like S_2 for ''pure'' totally impenetrable rods in thermal equilibrium [see (22)]. While we cannot conclude decisively from this graph the precise components of the laminate, we see that the structure of the laminate on both length scales is reflected in S_2.

III. EFFECTIVE CONDUCTIVITY TENSOR OF LAMINATES

A laminate with a finite separation of length scales has fields which are not piecewise uniform, and so its effective conductivity cannot be calculated analytically. We will use rigorous second-order bounds on $\boldsymbol{\sigma}_e$ that depend on S_2 (which was calculated in the previous section) and the phase conductivities σ_1 and σ_2 to estimate the effective conductivity for laminates with a finite separation of length scales. We verify that these bounds converge to the Hashin-Shtrikman bounds for macroscopically isotropic laminates, i.e., laminates that satisfy (6) and have an infinite separation of length scales.

A. Second-order contrast bounds

By taking certain Padé approximants of (3), Sen and Torquato [16] obtained bounds of arbitrary order on the effective conductivity tensor $\boldsymbol{\sigma}_e$. The second-order bounds on $\boldsymbol{\sigma}_e$ are given by

$$\frac{\boldsymbol{\sigma}_e}{\sigma_j}=\mathbf{I}+\frac{\phi_i(\sigma_i-\sigma_j)}{\sigma_j}\left[\mathbf{I}-\frac{1}{\phi_i}\frac{(\sigma_i-\sigma_j)}{\sigma_j}\mathbf{a}_2\right]^{-1}, \tag{28}$$

where $i,j=1,2$ and $i\neq j$ as before,

$$\mathbf{a}_2=\tfrac{1}{2}(\mathbf{A}_2-\phi_i\phi_j\mathbf{I}), \tag{29}$$

and $\mathbf{A}_2$ is given by (5). For $\sigma_2\geqslant\sigma_1$, we obtain a lower bound from (28) for $j=1$ and $i=2$, and we obtain an upper bound for $j=2$ and $i=1$.

We note in passing that one can eliminate the parameter $\mathbf{a}_2$ by utilizing the property that $\mathrm{Tr}\,\mathbf{a}_2=-\phi_i\phi_j$ (since $\mathbf{A}_2$ is traceless) to yield the simpler bounds on the eigenvalues λ_1 and λ_2 of $\boldsymbol{\sigma}_e$ obtained by Lurie and Cherkaev [3,9] and by Tartar [4]:

$$\frac{1}{\sigma_1}+\frac{1}{\lambda_1-\sigma_1}+\frac{1}{\lambda_2-\sigma_1}\leqslant\frac{1}{\phi_2}\left(\frac{1}{\sigma_1}+\frac{2}{\sigma_2-\sigma_1}\right), \tag{30}$$

$$\frac{1}{\sigma_2}+\frac{1}{\lambda_1-\sigma_2}+\frac{1}{\lambda_2-\sigma_2}\geqslant\frac{1}{\phi_1}\left(\frac{1}{\sigma_2}+\frac{2}{\sigma_1-\sigma_2}\right), \tag{31}$$

where $\sigma_2\geqslant\sigma_1$.

When $\mathbf{A}_2=\mathbf{0}$, the bounds (28) coincide with the Hashin-Shtrikman bounds on macroscopically isotropic two-phase composites, which are known to be optimal for several classes of composites. One such class is a geometry of space-filling, singly-coated circular cylinders [18], where the inner core is one phase and the outer shell is the other phase. Another example is the Vigdergauz construction [19]. Also, the bounds (28) are realized for $\mathbf{A}_2\neq\mathbf{0}$ by space-filling, singly coated ellipsoids [4,24,25].

Second-rank laminates with a wide separation of length scales have also been shown by macroscopic methods to achieve the bounds (28) and thus are optimal composites [3,4]. We conclude again that $\mathbf{A}_2$ must be the zero tensor for macroscopically isotropic laminates. However, this previous research does not determine $\mathbf{A}_2$ and hence the bounds (28) for laminates with a finite separation of length scales.

In order to quantify the degree of anisotropy of laminates with a finite separation of length scales, we introduce the parameter

$$\gamma=\frac{\max(|\Lambda_1|,|\Lambda_2|)}{\phi_1\phi_2}, \tag{32}$$

where Λ_1 and Λ_2 are the eigenvalues of $\mathbf{A}_2$. This is a purely microstructural parameter, independent of the conductivities σ_1 and σ_2. Since $-\phi_1\phi_2\leqslant\Lambda_1,\Lambda_2\leqslant\phi_1\phi_2$ [16], we see that $0\leqslant\gamma\leqslant1$. When $\gamma=0$, the system is macroscopically isotropic. However, when $\gamma=1$ (achieved by a system of aligned needles), the system is quite anisotropic. In the next section we will study the dependence of γ on the separation of length scales.

B. Calculation of bounds for laminates

We now directly calculate $\mathbf{A}_2$ for laminates with any separation of length scales by numerically integrating (5) using (13), and explicitly verify that $\mathbf{A}_2$ indeed tends to zero for second-rank laminates which obey (6) as the separation of length scales tends to infinity. While this result is expected, it is not at all obvious from the perspective of the microstructure since $S_2(r,\theta)$ is not symmetric about $\theta=\pi/4$ for laminates, as discussed in the Introduction. We then calculate bounds on the effective conductivity tensor using (28).

To begin our analysis, laminates are symmetric about $\theta=\pi/2$; therefore, in view of (5), the off-diagonal components of $\mathbf{A}_2$ are zero. Our calculation of $\mathbf{A}_2$ thus reduces to calculating only one of the diagonal components.

We now consider fully penetrable laminates with a wide separation in length scales and substitute (19) into (5) to calculate $\mathbf{A}_2$ asymptotically for fixed η_1 and η_2 as the separation of length scales $q=d_1/d_2\to\infty$. We find that

$$(\mathbf{A}_2)_{yy}=-\phi_1(1-2\phi_1^{(2)}+\phi_1)+O(\ln q/q) \tag{33}$$

as $q\to\infty$. Recall that $\phi_1^{(2)}$ is the volume fraction of phase 1 of the one-dimensional process which determined the second stage of lamination, which is

$$\phi_1^{(2)}=e^{-\eta_2}=e^{-\rho_2 d_2} \tag{34}$$

for fully penetrable laminates from (16). The calculation of (33) is described in Appendix C. We conclude from this asymptotic result that $\mathbf{A}_2$ tends to zero as the separation of length scales tends to infinity whenever (6) is satisfied. We also conclude that fully penetrable laminates with a wide separation of length scales achieve the anisotropic bounds of (28).

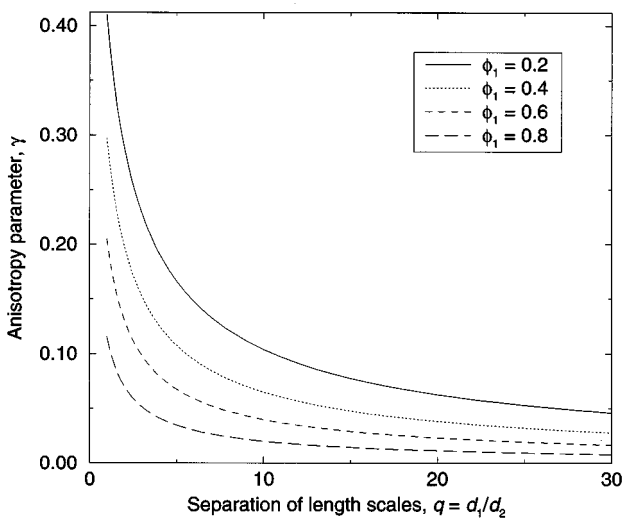

FIG. 5. The anisotropy parameter γ, given in (32), for laminates which satisfy (6) versus separation of length scales $q=d_1/d_2$, at several volume fractions ϕ_1 of the disconnected phase (phase 1). As expected, γ tends to zero as q tends to infinity. We see that $\gamma<0.05$ whenever $\phi_1>0.2$ and $q>30$.

We now numerically calculate $\mathbf{A}_2$ and hence γ for laminates with a finite separation of length scales. In Fig. 5 we plot numerical evaluations of γ for laminates which satisfy (6) at various ϕ_1 and q. We again see that $\gamma\to0$ as $q\to\infty$. We also see that, for constant q, γ decreases as ϕ_1 increases. This makes heuristic sense: for small ϕ_1, the laminate will resemble a system of aligned needles, while for large ϕ_1 there will be very few slabs in both the x and y directions, and hence the laminate will have similar structure in both directions.

From our numerical evaluation of $\mathbf{A}_2$, we now obtain bounds on $\boldsymbol{\sigma}_e$ by using (28). In Figs. 6, 7, and 8 we show the x and y components of $\boldsymbol{\sigma}_e$ for fully penetrable laminates of second rank which satisfy $\sigma_2/\sigma_1=10$ and (6) for $q=1$, 10 and ∞, respectively. We see that as the separation of length scales increases, the bounds in the x and y directions converge until they are identical and equal to the two-dimensional Hashin-Shtrikman bounds when the laminate is macroscopically isotropic. Using (28) and (13), we are also able to calculate bounds on $\boldsymbol{\sigma}_e$ for second-rank laminates of arbitrary construction.

When $d_1=d_2$, we see that the bounds on the effective conductivity in the x direction are somewhat smaller than the bounds in the y direction; in fact, for sufficiently small ϕ_1, the lower bound on $(\boldsymbol{\sigma}_e)_{yy}$ is larger than the upper bound on $(\boldsymbol{\sigma}_e)_{xx}$, regardless of which phase has a higher conductivity. A physical explanation of this phenomenon when the disconnected phase is a better conductor than the connected phase is trivial: even for very small ϕ_1, the volume fraction requirement (6) still requires that $\phi_1^{(2)}$ will be no smaller than 0.5. Therefore, the laminate will resemble a system of highly conducting needles aligned in the y direction. On the other

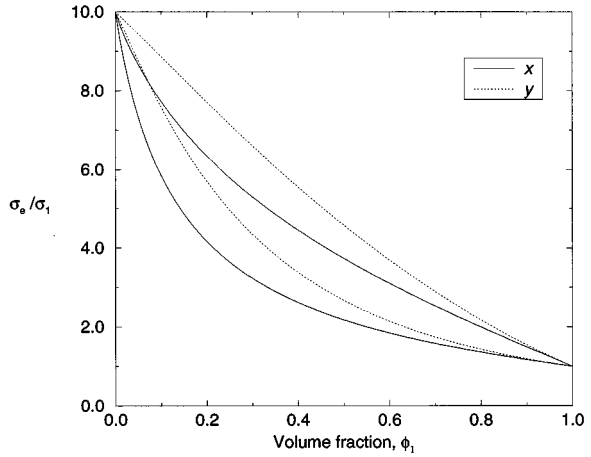

FIG. 6. The second-order bounds on the x and y components of the scaled effective conductivity σ_e/σ_1 for second-rank fully penetrable laminates in which $\sigma_2/\sigma_1=10$. Here σ_1 and σ_2 are the conductivities of phases 1 and 2, respectively. The laminates depicted in the above graph are determined by (6) and the length scale ratio $q=d_1/d_2=1$.

hand, if the slabs are better conductors, then current will be able to flow in the y direction in a straight line unimpeded, while current in the x direction will tend to flow around the needles. Such heuristic explanations, however, do not explain the behavior of the bounds for all possible length scales, phase conductivities and phase volume fractions.

IV. CONCLUSIONS

We have calculated S_n for fully penetrable laminates and S_2 for general laminates of arbitrary rank in terms of their constituent processes. We have explicitly given S_2 for three different types of second-rank laminates: fully penetrable, totally impenetrable, and random checkerboard. Using our expression for S_2, we have calculated the tensor coefficient $\mathbf{A}_2$ numerically for general second-rank laminates, thereby obtaining estimates on the effective conductivity tensor in the form of bounds. We have done this for laminates with an arbitrary separation of length scales. We have also explicitly verified that $\mathbf{A}_2$ indeed vanishes for optimal, macroscopically isotropic laminates, even though S_2 for laminates does not have symmetry about $\theta=\pi/4$.

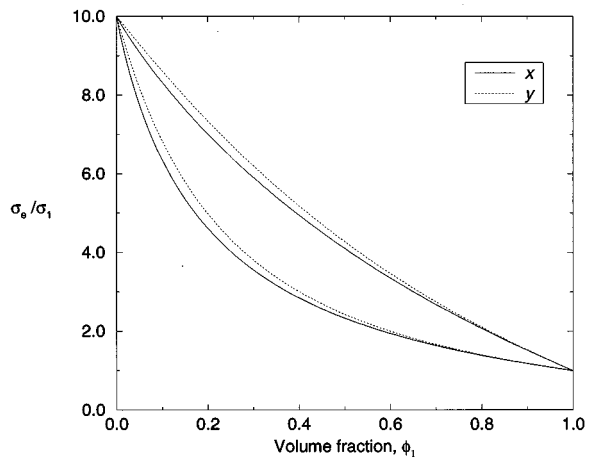

FIG. 7. As in Fig. 6, except $q=10$.

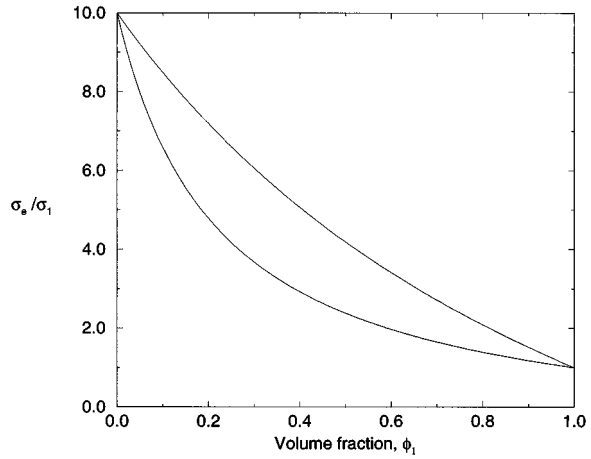

FIG. 8. As in Fig. 6, except $q=\infty$. Since we impose an infinite separation of length scales, the laminates are macroscopically isotropic and the bounds are independent of direction.

This last observation leads to the natural question raised in the Introduction: what symmetries must the S_n for optimal, macroscopically isotropic composites possess so that all of the tensor coefficients $\mathbf{A}_n^{(i)}$ vanish? This is a very difficult question to answer generally. We have shown explicitly that a sufficient condition for $\mathbf{A}_2$ to vanish is an S_2 of the form (13) for *any* choice of $S_2^{(1)}$, $L^{(1)}$, and $S_2^{(2)}$, as long as condition (6) is satisfied and the separation of length scales between the two stages tends to infinity. From (5), another sufficient condition is symmetry of S_2 about $\theta=\pi/4$. We have not shown, however, that these conditions are necessary. We have also not considered conditions which would ensure that the higher $\mathbf{A}_n^{(i)}$ vanish.

From a practical point of view, laminates with an infinte separation of length scales cannot be constructed. A natural question is thus determining how large the separation of length scales should be so that, for all intents and purposes, the laminate is an optimal structure. Judging by the convergence of the bounds, we suggest that a reasonable condition for declaring a second-rank laminate to be macroscopically isotropic is $\gamma<0.05$. This is achieved at most volume fractions when $q>30$.

ACKNOWLEDGMENTS

The authors thank Martin C. Carlisle for introducing them to the method of subtracted singularities and L. Gibiansky for many helpful discussions. This work was supported in part by the MRSEC Program of the National Science Foundation under Contract No. DMR-9400362, and by the U.S. Department of Energy, Office of Basic Energy Sciences under Grant No. DE-FG02-92ER14275. J.Q. acknowledges the National Science Foundation for financial support.

APPENDIX A: LINEAL PATH FUNCTION FOR SECOND-RANK LAMINATES

To characterize their microstructure, we determined S_n for laminates in Sec. II. We continue this characterization by

determining the lineal path function for second-rank laminates, i.e., the probability that the line connecting two points lies entirely in one of the phases. Using the independence of successive stages, the probability that the line between two points lies entirely in phase 1 is given by

$$L_1(x,y)=L^{(1)}(x)L^{(2)}(y). \tag{A1}$$

The corresponding probability for phase 2 is not nearly as trivial to calculate; a full expression for $L_2(x,y)$ would require knowledge of the joint distribution of the size of the clusters and the number of gaps in a given interval. However, in the y direction, the connected-phase lineal path function is given by

$$L_2(0,y)=\phi_2^{(1)}+\phi_1^{(1)}C_2^{(2)}(y), \tag{A2}$$

where $C_2^{(2)}$ is the two-point cluster function [26] for the second stage of lamination. In the x direction we have

$$L_2(x,0)=\sum_{r=0}^{\infty} N_r(x)(\phi_2^{(2)})^r, \tag{A3}$$

where $N_r(x)$ is the probability that, for the one-dimensional process which generates the first stage of lamination, a given interval of length x contains exactly r gaps (including gaps at the beginning and the end of the interval).

The probability N_r for fully penetrable rods was calculated by Domb [27]. In terms of the dimensionless distance $u=|x|/d_1$, where as before we take $j\leqslant u\leqslant j+1$, N_r is given by

$$N_0(u)=1+\sum_{k=0}^{j}(-1)^{k+1}\phi_1^{k+1}\left(\frac{[\eta(u-k)]^k}{k!}+\frac{[\eta(u-k)]^{k+1}}{(k+1)!}\right) \tag{A4}$$

for $r=0$ and by

$$N_r(u)=\sum_{k=0}^{j-r+1}(-1)^k\phi_1^{j+k}\binom{j+k}{k}\left(\frac{[\eta(u-j-k+1)]^{j+k-1}}{(j+k-1)!}+\frac{[\eta(u-j-k+1)]^{j+k}}{(j+k)!}\right) \tag{A5}$$

for $1\leqslant r\leqslant j+1$, while $N_r(u)=0$ otherwise. In these expressions η is again the reduced density defined by (15). In one dimension, the probability that a given interval has no gaps is the two-point cluster function C_2, which was independently calculated by Çinlar and Torquato [28]. Substitution of N_r into (A3) gives $L_2(x,0)$ for second-rank laminates whose first stage is generated by fully penetrable rods.

APPENDIX B: ASYMPTOTIC APPROXIMATION OF S_2 FOR HARD RODS IN EQUILIBRIUM

We develop an asymptotic approximation for $S_2(u)$ as the dimensionless distance $u\to\infty$ for a one-dimensional system of hard rods of unit diameter in equilibrium. This approximation is useful when numerically calculating $\mathbf{A}_2$ using (5).

To obtain this approximation, we find a generating function whose coefficients give $S_2(u)$. We then use the method of subtracted singularities to determine the asymptotic behavior of the coefficients [and hence $S_2(u)$] for large u.

We first state the main theorem behind the method of subtracted singularities [29,30].

Theorem. Let the function f be meromorphic for $|z|\leqslant R$ and analytic for $|z|=R$ and $z=0$, with simple poles inside this circle at z_i with residues c_i, $i=1,\ldots,m$. Then the coefficients f_n defined by

$$f(z)=\sum_{n=0}^{\infty} f_n z^n \tag{B1}$$

satisfy

$$f_n=-\sum_{k=1}^{m}\frac{c_k}{z_k^{n+1}}+O(R^{-n}). \tag{B2}$$

(This theorem can be generalized to functions with poles of finite order greater than one, but for the present purpose this generalization is not needed.)

To apply this theorem to the present problem, we restrict $0\leqslant y<1$ and define the sequence $\{a_j(y)\}$ by

$$a_j(y)=S_2(j+y). \tag{B3}$$

Recall that S_2 for hard rods in equilibrium is given by (22).

We now seek the generating function for this sequence, i.e., the function that satisfies

$$f(z;y)=\sum_{j=0}^{\infty} a_j(y)z^j. \tag{B4}$$

Straightforward algebraic manipulation verifies that this function is given by

$$f(z;y)=\frac{(1-\eta)\exp[(z-1)y/a]}{1-z\,\exp[(z-1)/a]}. \tag{B5}$$

Recall that a is defined by (23). To use the method of subtracted singularities to determine the asymptotic growth of the coefficients of f [and hence the growth of $S_2(j+y)$ as $j\to\infty$], we must first find the poles and associated residues of f. Clearly $z_0=1$ is a pole of f with residue

$$c_0 = -\frac{1-\eta}{1+1/a}. \tag{B6}$$

For $\eta<1$ there are no poles with modulus less than one. Therefore, as $u=j+y\to\infty$, (B2) implies that

$$S_2(u)\to\frac{1-\eta}{1+1/a}1^{-(j+1)} \text{ as } j\to\infty$$
$$=(1-\eta)^2. \tag{B7}$$

as expected. When $\eta=0.5$ this limit reduces to the remarkable identity

$$\lim_{j\to\infty}\sum_{k=0}^{j} e^{-k}\frac{k^{j-k}}{(j-k)!}=\frac{1}{2}. \tag{B8}$$

To determine the oscillations around the long-range value, other complex poles must be calculated numerically; they will depend on the value of η for the system. Every pole of f can be shown to be simple and the residue at a pole z is given by

$$c=-\frac{(1-\eta)\exp[(z-1)y/a]}{(1+z/a)\exp[(z-1)/a]}. \tag{B9}$$

In summary, once we have numerically calculated the poles of smallest modulus of f, we can use the above theorem and (B9) to determine the asymptotic behavior of $S_2(u)$.

To see how useful the above procedure is, we now take $\eta=0.5$. The first four nontrivial poles of f for this choice of η are approximately

$$z_{1,2}=-0.532092\pm 4.597158i \tag{B10}$$

and

$$z_{3,4}=-1.393982\pm 10.868006i, \tag{B11}$$

with residues

$$c_k=-\{\exp[(z_k-1)y]\}(0.489044\pm 0.107648i) \tag{B12}$$

for $k=1,2$ and

$$c_k=-\{\exp[(z_k-1)y]\}(0.501655\pm 0.0459462i) \tag{B13}$$

for $k=3,4$. We now substitute these values into (B2) and compare with the exact result of (22) for $\eta=0.5$. We see in Fig. 9 that this ''asymptotic'' expression is in fact very close to the actual value of $S_2(u)$ for small u using only the first four nontrivial poles. We also can use this expression for S_2 at large distances to accurately and quickly calculate the integrand of (5) when calculating $\mathbf{A}_2$ for totally impenetrable laminates.

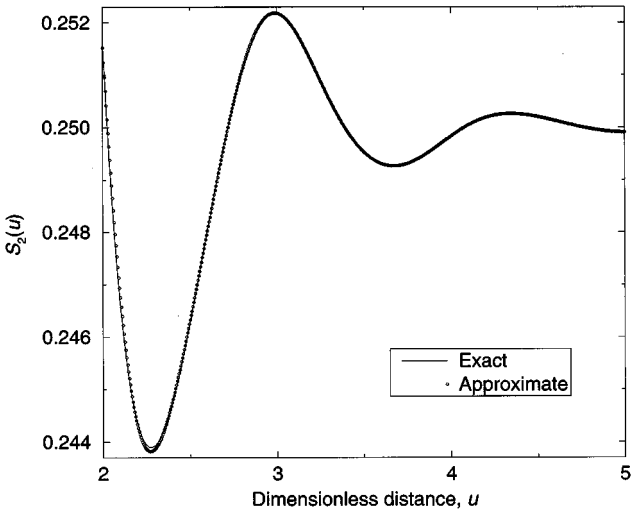

FIG. 9. Exact graph of the two-point probability function $S_2(u)$ for totally impenetrable rods in thermal equilibrium and its asymptotic approximation using the first four nontrivial poles. The reduced density of the system of rods is $\eta=0.5$. The approximation is very close to the exact result even for small values of the dimensionless distance u.

APPENDIX C: ASYMPTOTIC BEHAVIOR OF A_2 FOR LAMINATES WITH A WIDE SEPARATION OF LENGTH SCALES

We discuss how (33) can be derived for fully penetrable laminates. Combining (19) and (5), we find that, when $d_1>2d_2$,

$$(\mathbf{A}_2)_{yy}=I_1+I_2+I_3+I_4+I_5, \tag{C1}$$

where

$$I_1=\frac{4}{\pi}\int_{d_2}^{\infty}\int_0^{d_1}\frac{y^2-x^2}{(x^2+y^2)^2}(e^{-\rho_1(x+d_1)-2\rho_2 d_2}-\phi_1^2)dx\,dy, \tag{C2}$$

$$I_2=\frac{4}{\pi}\int_0^{d_2}\int_{d_1}^{\infty}\frac{y^2-x^2}{(x^2+y^2)^2}\phi_1 e^{-\rho_1 x}(e^{-\rho_2 y}-e^{-\rho_2 d_2})dx\,dy, \tag{C3}$$

$$I_3=-\frac{4}{\pi}\lim_{\delta\to 0}\int_{\delta}^{d_2}\int_0^{\pi/2}\frac{\cos 2\theta}{r}(e^{-\rho_1 r\cos\theta-\rho_2 r\sin\theta}-\phi_1^2)d\theta\,dr, \tag{C4}$$

$$I_4=\frac{4}{\pi}\int_0^{d_2}\int_{\sqrt{d_2^2-y^2}}^{2d_2}\frac{y^2-x^2}{(x^2+y^2)^2}(e^{-\rho_1 x-\rho_2 y}-\phi_1^2)dx\,dy, \tag{C5}$$

and

$$I_5=\frac{4}{\pi}\int_0^{d_2}\int_{2d_2}^{d_1}\frac{y^2-x^2}{(x^2+y^2)^2}(e^{-\rho_1 x-\rho_2 y}-\phi_1^2)dx\,dy. \tag{C6}$$

We have converted to rectangular coordinates for each of these expressions except I_3. We have also used the symmetry of S_2 to calculate $\mathbf{A}_2$ in terms of integrals on the first quadrant.

As $q=d_1/d_2\to\infty$ for fixed η_1 and η_2, we use the dominated convergence theorem [31] to replace the integrands by a series in $1/q$; depending on the domain we expand either the exponential term or the term $(y^2-x^2)/(x^2+y^2)^2$. Evaluation of the resulting integrals yields (33).

A similar analysis shows that (33) is satisfied for laminates constructed by one-dimensional random checkerboards. In fact, since all laminates with an infinite separation of length scales must achieve the Padé bounds on effective conductivity, (33) must be true to leading order, regardless of how the laminate is constructed. This is not at all obvious from the perspective of the microstructure.

[1] R. M. Christensen, *Mechanics of Composite Materials* (Wiley, New York, 1979).

[2] S. Torquato, Appl. Mech. Rev. **44**, 37 (1991).

[3] K. A. Lurie and A. V. Cherkaev, Proc. R. Soc. Edinburgh **99A**, 71 (1984); Adv. Mech. (Poland) **9**, 3 (1986).

[4] L. Tartar, in *Ennio de Giorgi Colloquium*, edited by Paul Krée (Pitman, Boston, 1985), pp. 168–187.

[5] G. W. Milton, in *Homogenization and Effective Moduli of Materials and Media*, edited by J. L. Erickson *et. al.* (Springer-Verlag, New York, 1986), pp. 150–174.

[6] G. A. Francfort and F. Murat, Archive Rat. Mech. Analysis **94**, 307 (1986).

[7] G. W. Milton and R. V. Kohn, J. Mech. Phys. Solids **36**, 597 (1988).

[8] A. N. Norris, Mech. Mat. **4**, 1 (1985).

[9] K. A. Lurie and A. V. Cherkaev, Ioffe Institute Report No. 895, 1984 (unpublished); J. Opt. Theor. Appl. **46**, 571 (1985).

[10] M. Avellaneda, SIAM J. Appl. Math. **47**, 1216 (1987).

[11] R. V. Kohn and R. Lipton, Archive Rat. Mech. Analysis **102**, 331 (1988).

[12] E. Baer, A. Hiltner, and R. J. Morgan, Physics Today **45**, 60 (1992).

[13] S. A. Wainwright, W. D. Boggs, J. D. Currey, and J. M. Gosline, *Mechanical Design in Organisms* (Princeton University Press, Princeton, NJ, 1982), p. 81.

[14] J. D. Currey, *The Mechanical Adaptation of Bones* (Princeton University Press, Princeton, NJ, 1984).

[15] M. Sarikaya and I. A. Aksay, in *Cellular Synthesis and Assembly of Polymers*, edited by S. Case (Springer-Verlag, New York, 1992), p. 1.

[16] A. K. Sen and S. Torquato, Phys. Rev. B **39**, 4504 (1989).

[17] S. Torquato and A. K. Sen, J. Appl. Phys. **67**, 1145 (1990).

[18] Z. Hashin and S. Shtrikman, J. Appl. Phys. **33**, 3125 (1962); Z. Hashin, in *Mechanics of Composite Materials* (Pergamon Press, New York, 1970).

[19] S. B. Vigdergauz, J. Mech. Phys. Solids **42**, 729 (1994); ASME J. Appl. Mech. **61**, 390 (1994).

[20] S. Torquato and G. Stell, J. Chem. Phys. **77**, 2071 (1982).

[21] B. Lu and S. Torquato, Phys. Rev. A **45**, 922 (1992).

[22] S. Torquato and G. Stell, J. Chem. Phys. **79**, 1505 (1983).

[23] S. Torquato and F. Lado, J. Phys. A **18**, 141 (1985). There is a typographical error in (3.4) of this reference; the third case should be $\sigma-a+A(r)-2B(r)+C(r)$.

[24] G. W. Milton, in *Advances in Multiphase Flow and Related Problems*, edited by G. Papanicolaou (SIAM, Philadelphia, 1986), p. 136.

[25] G. W. Milton, J. Appl. Phys. **52**, 5286 (1981).

[26] S. Torquato, J. D. Beasley, and Y. C. Chiew, J. Chem. Phys. **88**, 6540 (1988).

[27] C. Domb, Proc. Camb. Phil. Soc. **43**, 329 (1947).

[28] E. Çinlar and S. Torquato, J. Stat. Phys. **78**, 827 (1995).

[29] P. Flajolet and R. Sedgewick, Institut National de Recherche en Informatique et en Automatique Report No. 2026, 1993 (unpublished).

[30] P. Henrici, *Applied and Computational Complex Analysis* (Wiley, New York, 1977), Vol. 2, pp. 442–446.

[31] H. Royden, *Real Analysis*, 3rd ed. (Macmillan, New York, 1988), p. 267.